Atmospheric Environment 45 (2011) 5138–5149

Contents lists available at ScienceDirect

Atmospheric Environment

journal homepage: www.elsevier.com/locate/atmosenv

Size distribution of atmospheric aerosols at Maitri, Antarctica

Vimlesh Pant [1], Devendraa Siingh*, A.K. Kamra

Indian Institute of Tropical Meteorology, Pune, India

ARTICLE INFO

Article history:
Received 11 January 2011
Received in revised form
26 May 2011
Accepted 10 June 2011

Keywords:
Antarctic aerosols
Aerosol size distribution
Nucleation mode particles
Marine aerosols

ABSTRACT

Measurements of the concentration and size distribution of the atmospheric aerosol particles in the size range of 0.003–20 μm diameter have been made at Maitri (70°45′52″S, 11°44′03″E) during January–February, 2005. The measured particle size ranges extended from 0.5 to 20 μm throughout the period, from 0.016 to 0.7 μm in January and 0.01 to 0.4 μm in February. For short intervals of time, comprising a total period of 210 h, the measurements were made for particles in the size range of 0.003–0.16 μm. Total particle number concentrations of coarse and fine particles vary from 0.1 to 0.8 and from 100 to 2000 particles cm^{-3}, respectively. The fine particle concentration undergoes a diurnal variation with values remaining low (300–400 cm^{-3}) during low sun periods and increasing up to ~750 cm^{-3} at noontime. The monthly-averaged number size distributions show maxima in accumulation mode at 0.772 ± 0.023 μm, in Aitken mode at 0.089 ± 0.005 μm in January which shifts to 0.03 ± 0.003 μm in February, and in nucleation mode at 0.018 ± 0.002 μm. The hourly-averaged curves can have one mode each in coarse, accumulation, and nucleation size ranges, and two modes in Aitken size range of particles. Total number concentration of particles in coarse mode is higher in oceanic than in continental air masses. Further, while the oceanic air masses have nucleation mode at 0.01 μm and Aitken mode at 0.024 μm, continental air masses have nucleation mode at 0.017 μm. Intermixing of the two air masses at coastal site results in multi-modal size distributions. It is inferred that while in continental air masses the nucleation mode particles are aged, in oceanic air masses these are likely to be transported from the upper troposphere under subsidence of cyclonic storms revolving around the continent of Antarctica.

1. Introduction

Atmospheric aerosol particles can significantly affect the radiative balance of the Earth, both directly, through scattering and absorption of the short and long-wave radiations (Charlson et al., 1992) and indirectly, by acting as condensation nuclei, thereby enhancing the liquid water content and lifetime of the clouds (Twomey, 1974; Squires, 1958; Albrecht, 1989). They may also influence the heterogeneous chemistry of the atmosphere (Schwartz et al., 1996). Over the continent of Antarctica where ~98% of the surface is covered with snow and ice and the surface albedo can exceed 0.85, the aerosols, especially the absorbing particles suspended over the bright surface can make significant changes in radiative forcing in those regions (Chylek and Coakley, 1974; Randles et al., 2004). Large spatial and temporal variabilities in the composition and the physical and chemical characteristics of aerosols over the continent of Antarctica further adds to the complications of estimating such changes in radiative forcing. Understanding these changes to estimate the radiation budget of the atmosphere has become important in recent times in view of the decreasing polar albedo due to decrease in sea-ice and snow cover areas (de la Mare, 1997; Holland et al., 2006).

Intermixing of the continental and marine air-masses makes it difficult to understand the physical and chemical characteristics of the atmospheric aerosols over a coastal station. Temporal and spatial variabilities of air circulation over such regions further complicate the problem of understanding aerosol properties and in identifying the sources and sinks of aerosols. The complexity of the problem is somewhat reduced if such measurements are made at a coastal station in Antarctica where effects of anthropogenic pollution can be neglected, atmosphere is much cleaner and the air circulation is more organized and persistent (e.g. Parish, 1988; Ito, 1993).

At an Antarctic coastal station, the atmospheric aerosols are mainly generated by the gas-to-particle conversion of oxidation products of precursor gases emitted by the ocean and by the

* Corresponding author.
E-mail addresses: devendraasiingh@tropmet.res.in, dvendraasiingh@gmail.com (D. Siingh).
[1] Present address: Aryabhatta Research Institute of Observational Sciences, Nainital, India.

1352-2310/$ – see front matter © 2011 Elsevier Ltd. All rights reserved.
doi:10.1016/j.atmosenv.2011.06.028

bursting of air bubbles on the ocean surface (Minikin et al., 1998). These particles are removed from the atmosphere through gravitational deposition and precipitation scavenging (Kerminen et al., 2000; Hara et al., 2005, 2006). Further, while suspended in the air, their sizes are transformed through the processes of coagulation, condensation of low volatility gases and cloud processes (Hoppel et al., 1994). As a consequence of different contributions of these processes under the changing meteorological conditions at coastal stations, aerosol characteristics exhibit a variety of temporal and spatial variations. Periodic number size distributions measurements at Antarctica are also important to monitor long term changes in background aerosol concentration since a small change in it may lead to large changes in global atmospheric processes which contribute to global climatic changes (Charlson et al., 1987).

Importance of atmospheric process and associated size-related properties of aerosols, such as new particle formation (Kulmala et al., 2004), sulphur chemistry (Jourdain and Legrand, 2001), formation of sea-salt aerosols from fractionation of sea-ice (Wagenbach et al., 1998; Wolff et al., 2003), vertical transport of Aitken particles associated with cyclonic storms revolving around the continent of Antarctica (Pant et al., 2010), and long-range transport from the midlatitudes (Yamazaki et al., 1989; Hara et al., 2004) in Antarctic environment has been increasingly recognized in recent years. To assess the impact of aforementioned processes on aerosol properties in Antarctica, measurements of aerosol size distribution with higher size-resolution and finer time-average step are needed. Several investigators have studied different properties of Antarctic aerosols such as their chemical nature (e.g. Savoie et al., 1993; Minikin et al., 1998; Wagenbach et al., 1998; Kerminen et al., 2000), their total number and/or mass concentrations and size distributions (e.g. Samson et al., 1990; Jaenicke et al., 1992; Mazzera et al., 2001; Koponen et al., 2003; Deshpande and Kamra, 2004); their optical properties (Bodhaine et al., 1986); their role as cloud condensation nuclei (De Felice et al., 1997); and their chemical mass size distributions (e.g. Harvey et al., 1991; Gras, 1993; Ito, 1993; Teinila et al., 2000; Rankin and Wolff, 2003; Park et al., 2004; Virkkula et al., 2006). While fine particles of sulphate are most abundant over the Antarctic continent, coarse particles of sea-salt are major contributor to aerosols in the coastal Antarctic regions (Hall and Wolff, 1998; Wagenbach et al., 1998; Kerminen et al., 2000). The cyclonic storms revolving around the continent bring the marine air and aerosol particles in to the interior of the continent (Ito and Iwai, 1981; Pant et al., 2010). Size-segregated chemical composition of the Antarctic aerosols can provide the contribution of different substances to the aerosol particles in various size ranges at both coastal and continental sites (Minikin et al., 1998; Kerminen et al., 2000; Teinila et al., 2000; Koponen et al., 2003; Hara et al., 2004, 2005; Virkkula et al., 2006; Tomasi et al., 2007). The small nucleation mode particles generated in the Antarctic environment can grow to the size of accumulation mode category and, in addition to the hygroscopic salt particles, can act as cloud condensation nuclei (De Felice et al., 1997; Pant et al., 2010). Measurements in most of these studies which involve number or mass size distributions at the Antarctic coastal sites, have not spannedover five orders of magnitude of size range of atmospheric aerosol particles (Table 1). Particularly, the data on the nucleation and coarse mode particles are few and are needed to understand the contributions of various sources and sinks of the coastal aerosols at Antarctica. In this study, particles have been categorized in nucleation mode ($d < 0.02$ μm), Aitken mode ($0.02 < d < 0.1$ μm), accumulation mode ($0.1 < d < 1.0$ μm) and coarse mode ($d > 1$ μm).

In order to understand the nature and temporal variability of aerosols at a coastal station, Maitri (70°45′52″S, 11°44′03″E, 130 m above sea level) in Antarctica, we present here our measurements of the concentration and size distribution of atmospheric aerosol particles in the size range of 0.003–20 μm diameters made at finer time-resolution from January 1 to February 28, 2005 during the 24th Indian Scientific Expedition to Antarctica. Results are compared to the earlier measurements made at Maitri and elsewhere.

2. Instrumentation

A variety of instruments have been used in the past studies for measurements of the size distribution of aerosol particles at Antarctica. Previous particle size distribution measurements have been conducted with in-situ instruments as well as by off-line analysis (Shaw, 1986, 1988; Ito, 1993; Gras, 1993; Hall and Wolff, 1998; Kerminen et al., 2000; Virkkula et al., 2006; Jourdain et al., 2008). A number of techniques have been used to reliably measure the particle size distribution of Antarctic aerosols, for example, impactors (Hogan, 1979; Shaw, 1986, 1988; Lal and Kapoor, 1989), diffusion pipes (Gras and Adriaansen, 1985; Gras, 1993), electrical aerosol analyzer (Deshpande and Kamra, 2004) etc. The aerosol size distribution measurements with a combination of SMPS and APS employed in this study has two specific

Table 1
Past observations at Antarctic coastal sites.

Investigators	Location	Size-range (diameter)	Instrumentation	Remarks
Radke and Lyons (1982)	Ross sea region of coastal Antarctica	0.1–5 μm	OPC	Mean of measurements made near surface over the Ross sea, Antarctica
Harvey et al. (1991)	Butter PT. (77°40′S, 164°12′E)	0.12–3.12 μm	ASASP	Mean of measurements made between November 6–26, 1988
Jaenicke et al. (1992)	George von Neumayer (70°37′S, 8°22′W)	0.003–0.4 μm	CNC	Mean of measurements during 1982–1989
Ito (1993)	Syowa (69°00′S, 39°35′E)	0.004–2 μm	Pollak counter and diffusion pipes, OPC	Mean of measurements made in December month in 1978
Gras (1993)	Mawson (67°36′S, 62°53′E)	0.003–1 μm	Nolan-Pollak counter, diffusion battery	Mean of measurements from January 1 to February 18 for period 1985–1990
Koponen et al. (2003)	Aboa (73°03′S, 13°25′W)	0.003–0.8 μm	CPC, DMPS	Mean of measurements made between January 5–22, 2000 and January 1–26, 2001
Deshpande and Kamra (2004)	Maitri (70°45′S, 11°44′E)	0.003–1 μm	EAA	Mean of measurements made during January–February, 1997
Present study	Maitri (70.76°S, 11.73°E)	0.003–20 μm	SMPS, APS	Mean of measurements made during January–February, 2005

CNC-condensation nuclei counter, SMPS-scanning mobility particle sizer, APS-aerodynamic particle sizer, OPC-optical particle counter, ASASP-active scattering aerosol spectrometer probe, EAA-electrical aerosol analyzer, DMPS-differential mobility particle sizer, CPC-condensation particle counter.

advantages over other techniques, studying aerosols with finer size- and time-resolution (Koponen et al., 2003; Pant et al., 2010).

In the present study, measurements of total number concentration and number size distributions of aerosol particles in the size ranges of 0.003–0.7 μm and 0.5–20 μm were simultaneously made with finer time-resolution steps using the Scanning Mobility Particle Sizer (SMPS, TSI Model 3936) along with a butanol-based Ultrafine Condensation Particle Counter (UCPC) (TSI Model 3025A) and the Aerodynamic Particle Sizer (APS, TSI Model 3321), respectively. SMPS can measure concentrations from 20 to 10^7 particles cm^{-3} and has resolution of up to 64 geometrically equal channels per decade of particle size. It can complete a cycle of measurement in less than 10 min. APS can measure maximum particle concentrations of 1000 particles of 0.5 μm diameter with <2% coincidence and of 10 μm diameter with <6% coincidence. It has resolution of 32 channels per decade (total 50 channels) of particle size. The measurement cycle for the whole size range is 10 min. We assume that all particles have spherical shape, so both aerodynamic and electrical mobility diameters measured by APS and SMPS, respectively, are considered to be volume equivalent (Peters et al., 2006). Both instruments were kept inside the Kamet observatory which is located approximately 300 m upwind of the living modules and generator complex of Maitri station. Fig. 1a shows locations of Maitri and other stations at Antarctia along with a map of Maitri station (Fig. 1c) showing positions of Kamet hut and other structures.

The ambient air for the SMPS and APS were sampled through two conductive silicone inlet tubes of 0.5 cm internal diameter each and 1.0 m and 0.6 m length, respectively. Both tubes were projected out through a wall of the Kamet hut such that the inlets were located 0.2 m away from the wall and 2 m above the ground surface. The air was sampled at flow rates of 3.3/6.6 lpm and 5 lpm for the SMPS and APS, respectively. Flow rate in SMPS was switched over from 3.3 lpm to 6.6 lpm to change the measured particle diameter range from 0.0044–0.168 μm to 0.0031–0.11 μm. For diffusion coefficient of 3.23×10^{-3} and 1.38×10^{-8} cm^2 s^{-1} for 0.003 and 20 μm diameter particles, respectively, density of wet sea-salt particle as 1200 kgm^{-3} and viscosity of air as 1.8×10^{-5} Pa s, The loss of aerosol particles by diffusion/impaction to the walls of intake tube, as calculated from Fuchs (1964) formulae, were less than 15%/1% for 0.003 μm particles and ~2%/10% for 10 μm particles. The inlets were cleaned with butanol and allowed to dry, at least once a day to avoid accumulation of sea-salt, dust or snow in the inlet. The instruments were operated daily except during periods of heavy snowfall and blizzard. Measurements were made almost continuously from January 1 to February 28, 2005 and 10-min averaged samples were stored in a computer. Both, the SMPS and APS measurements covered 0.5–0.7 μm size range. However,

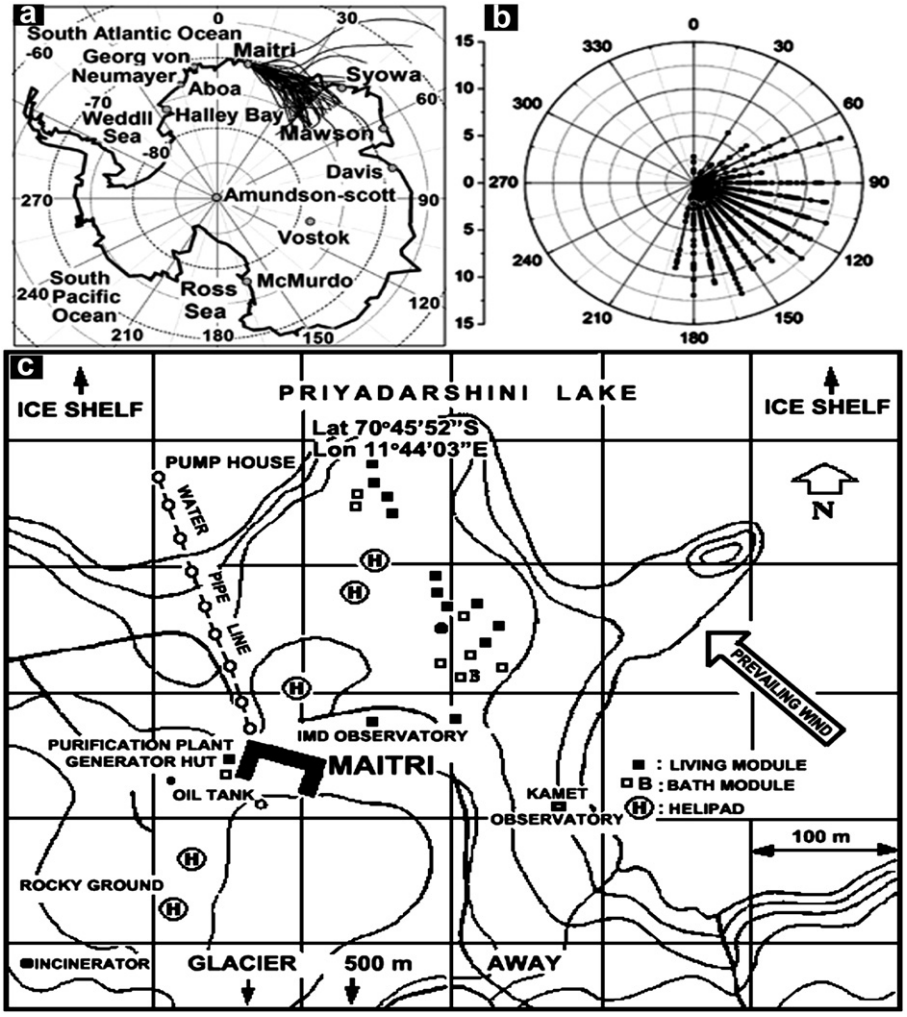

Fig. 1. Locations of Maitri and other stations at the continent of Antarctica and the daily 2-day back trajectories of air mass reaching Maitri at 0000 UT during January–February, 2005 (a). The wind-rose diagram of hourly surface winds at Maitri for the period of observations (b). Map of Maitri station showing positions of Kamet hut and other structures (c).

APS is known to underestimate the number concentration in this overlapping size range (Hoppel et al., 1985; Pant et al., 2008). This is because the two instruments are based on different principles of counting the particles. While the SMPS is based on the principle of the measurement of the electrical mobility, the APS is based on the optical technique for particle detection. The calibration of APS is very sensitive to the particle's refractive index. Refractive index of atmospheric particles is unknown and is likely to vary with time and from one location to the other. The manufacture's calibration with latex spheres is used for measurements. The measurements made with SMPS are inherently more accurate than those of APS. In order to explain the difference, Hoppel et al. (1985) found that electromagnetic extinction calculated from the size distribution agree better with the measured scattering when the mobility analyzer data was given more weight than the optical measuring data in the overlap area. In our collections of total particle concentration, we used the SMPS measurements in the overlapping region.

Both APS and SMPS systems were operated simultaneously. The APS system measured the particles in the size range of 0.5–20 μm diameter throughout the period. The SMPS measurements with the LDMA were collected nearly continuously, with periodic interruptions for measurements with the NDMA. The LDMA measurements were conducted for the size range of 0.016–0.7 μm diameter in January and subsequently 0.01–0.4 μm diameter in February since the particle concentrations near to the smaller end of this size range kept increasing. The measurements with the NDMA provided particle size distribution in the range of 0.003–0.16 μm diameter, and such measurements were collected for a total of 210 h to catch some events of new particle formation associated with convective storms revolving around the continent of Antarctica (Pant et al., 2010).

A Gerdiens Ion Counter Battery (GICB) consisting of three Gerdiens condensers, was being operated at Maitri for ion concentration measurements. GICB was manually operated for two days in mobility-measuring mode to get the ion-mobility spectra in the range of $2.29–2.98 \times 10^{-4}$ cm^2 v^{-1} s^{-1}. These data can be reduced to get aerosol particle size distribution in the 0.41×10^{-3}–0.109 μm diameter particles (Tammet, 1995). Detailed description of GICB is given by Dhanorkar and Kamra (1991) and Siingh et al. (2005, 2007, in press).

The meteorological parameters including air temperature, pressure, and wind speed and direction, were measured at 5 m above the ground level. Cloud coverage was estimated from the hourly visual observations of sky and was estimated in octas (1 octa being equal to 1/8th of the sky being covered with clouds). The air mass back trajectories were calculated using the NOAA HYSPLIT 4 model (Draxler and Hess, 1998; Draxler and Rolph, 2003).

3. Measurement site and weather

Fig. 1c shows the location of Maitri in Schirmacher oasis of the Drowning Maud Land in east Antarctica. The east-west trending Schirmacher oasis is exposed over an area of 35 km^2 and is covered by sandy and loamy sand types of soil. Large wind speeds are required to strip-off sand particles from the surface, especially when it is wet (Bagnold, 1965). No dust particles were normally observed to be airborne unless wind speed exceeded ~15 m s^{-1}. Maitri has steep cliffs, frozen lakes and an ice-shelf extending to about 90 km in the summer on the northern side, and polar ice and ice–rock interface that fluctuates with the season on the southern side. The ice-melt region existed on both the northern and southern sides of Maitri at a distance of about 0.5 km in this season. Cliffs on the northern side were not high and close enough to the station to block the oceanic air from reaching the observatory.

Fig. 1b shows a wind-rose of hourly surface winds recorded by the India Meteorological Department. All measurements were sampled at a height of 5 m above the ground at Maitri for the period of observations. Inspite of large variability in wind speed, the winds were dominantly southeasterly and 2-days back trajectories plotted in Fig. 1a showed that air masses approached Maitri from the southeast direction except during the periods when cyclonic storms passed close to Maitri. This minimized the chances of the observation site to be influenced by any emission from Maitri station. Fig. 2 shows the variations in various meteorological parameters. Unfortunately, measurements of relative humidity were not available. During this period, the mean values of air temperature and atmospheric pressure at Maitri were 0.08 ± 2.85 °C and 969 ± 8 hPa. Several dips recorded in the atmospheric pressure were mostly associated with the sub-polar low-pressure systems revolving around the continent of Antarctica between 65°S and 70°S. Under the influence of these eastward propagating low-pressure systems, the cloud cover generally showed alternating sequence of clear sky changing over to overcast and then again clearing as the system moved away. Two such low-pressure systems on Days 33 and 56 produced surface pressure drops of 20 and 30 hPa, respectively at Matiri.

An examination of the 5-day back trajectories at 00 UT (Supplementary Figure SF-1) showed that the air mass reaching Maitri before February 16, 2005 (Day 47) was always continental and came down as drainage from the polar ice in the elevated southern latitudes. After February 16, 2005, although the air masses still approached Maitri from east or southeast direction (as illustrated in Fig. 1a also), their backward trajectories show that air mass

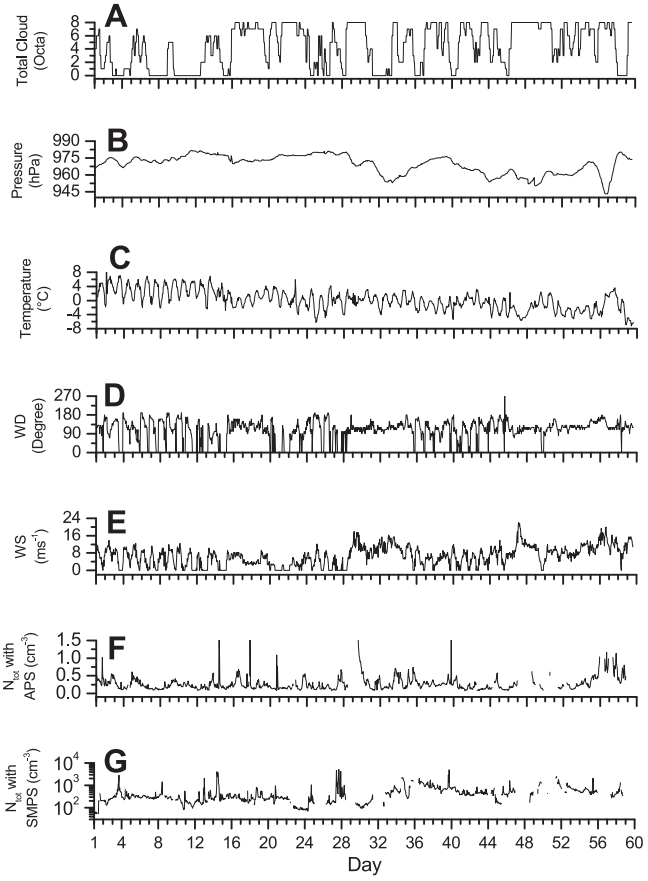

Fig. 2. Variations in various meteorological parameters and total number concentration of coarse and fine. N_{tot} – total number concentration, WS – wind speed, WD – wind direction.

originated, over ocean for more than 50% of the time and descended to Maitri from 500 to 3500 m altitude. So any chance of particle reaching at the measurement site from any anthropogenic source at Maitri was almost nil.

4. Observations

4.1. Total number concentration (TNC) of aerosol particles

A total of 7356 number size distributions with the APS and 6834 with the SMPS were measured during entire field campaign. Fig. 3 shows time series of particles in PM_{10} (as measured with the APS) and PM_1 (as measured with the SMPS) size categories measured at Maitri throughout the campaign period.

Each number size distribution was integrated to separately compute TNC in PM_{10} and PM_1 categories. These values of TNC are plotted in Fig. 2F and G, respectively. Very low mean values of TNC of 0.27 ± 0.20 particles cm^{-3} characterized our observations in PM_{10} (0.5–20 μm diameter) category during this period. On the other hand, the mean values of TNC PM_{10} category (0.003–0.7 μm diameter) were 321 ± 453 particles cm^{-3} in January and 670 ± 414 particles cm^{-3} in February. Temporal variations of particles in these two categories were not always similar, indicating two different sources for origin of particles in the two size ranges. 2-days back trajectories shown in Fig. 1a for this period support the view that these sources can be assumed as of combined continental or marine origin. Particle concentration in PM_{10} category was 2–4 orders of magnitude smaller than those in PM_1 category. The condensation nuclei concentrations of the same order had also been observed in this season at several other Antarctic coastal stations such as Syowa (69°S, 39.6°E), Mawson (67.6°S, 62.9°E), Ross Island (77.8°S, 166.8°E) and Georg-von-Neumayer (72.6°S, 8.4°W); (Ito, 1993; Jaenicke and Stingl, 1984; Gras and Adriaansen, 1985; Shaw, 1986; Lal and Kapoor, 1989; Jaenicke et al., 1992; Gras, 1993; Deshpande and Kamra, 2004). Measurements of Koponen et al. (2003) at Aboa (73°03′S, 13°25′W), about 150 km from the coast, also showed similar aerosol concentrations indicating that the ocean is a major source of atmospheric aerosols. The coarse particles play critical roles in some characteristics of the atmosphere. For example, coarse particles are dominant mass compared to fine mode particles in atmosphere and thus chemical properties of the atmosphere are almost totally determined by the coarse particles. Further, the coarse particles are important in understanding long-range transport of aerosols in Antarctica (Shaw, 1986; Jaenicke et al., 1992).

The PM_1 concentration in our observations showed a diurnal variation with values remaining low (<400 cm^{-3} in January and <600 cm^{-3} in February) during 2100 to 0800 UT and increasing up to 580 cm^{-3} in January and 960 cm^{-3} in February in the afternoon (Fig. 4). On the other hand, PM_{10} concentrations did not show much of the variability. Diurnal variation of the condensation nuclei concentration has also been reported at some other coastal stations e.g. Mawson, Georg-von-Neumayer and even at South Pole station, Amundsen-Scott (Hogan, 1979; Gras and Adriaansen, 1985; Jaenicke et al., 1992). Further analysis of our data reported in the next section shows that diurnal variation in PM_1 particles is mainly due to particles of <0.1 μm diameter.

4.2. Peaks in TNC

Time-variation of TNC of particles during this period showed some peaks (enhanced value of concentrations) which sometimes even exceeded 1.2 particles cm^{-3} in case of PM_{10} and 5000 particles cm^{-3} in case of PM_1. These peaks mostly lasted over

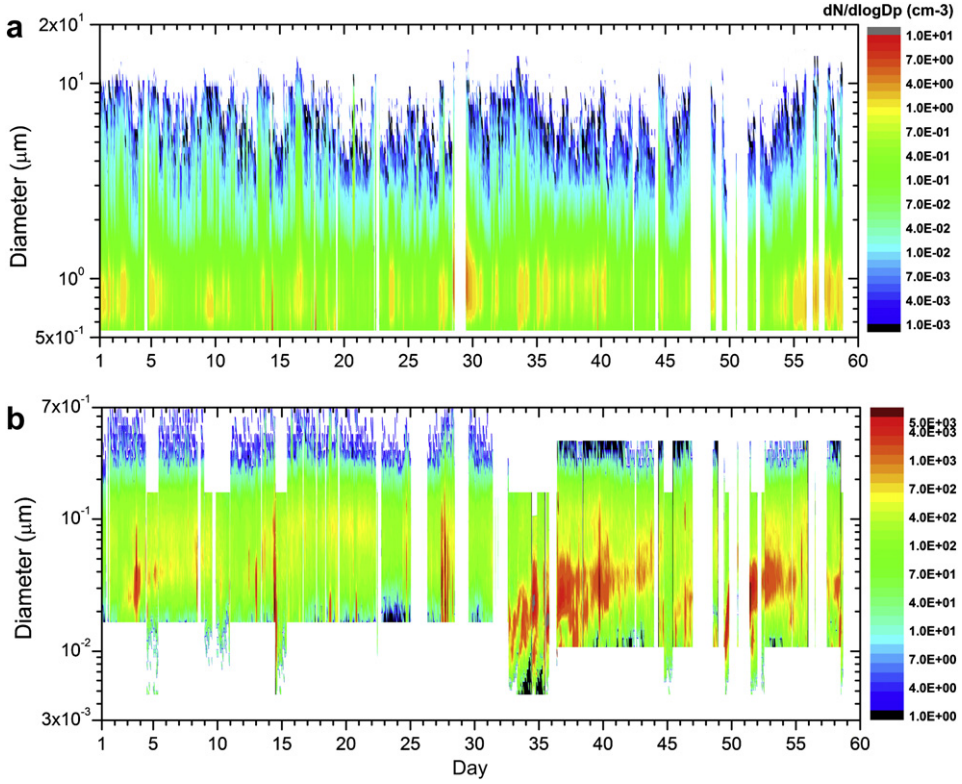

Fig. 3. Time series of particles in PM_{10} (as measured with the APS) (a) and PM_1 (as measured with the SMPS) (b) size categories measured at Maitri from January 1 to February 28, 2008. Gaps in data are because of the non-availability of data in those periods due to adverse weather conditions or for making arrangements for change of the measured size range or for cleaning the instruments.

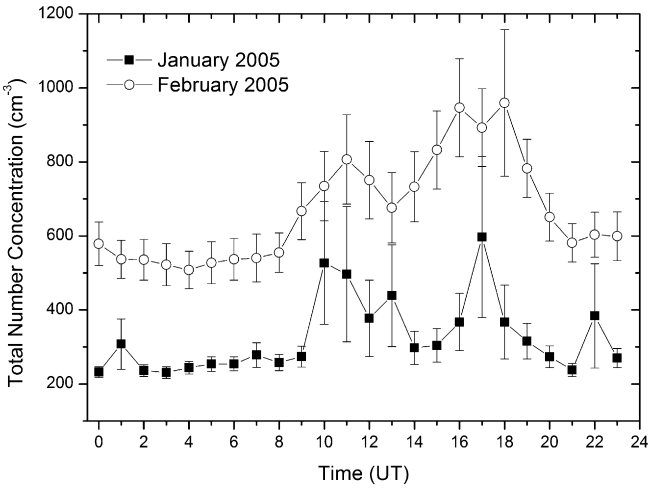

Fig. 4. Diurnal variation of fine particles at Maitri during January–February, 2005. Vertical bars show standard errors.

a period of a few tens of minutes and did not always occur simultaneously in PM_{10} and PM_1 category. The changes associated with the passage of the cyclonic storms revolving around the continent of Antarctica last over a few hours or days and they are discussed in detail elsewhere (Pant et al., 2010).

Out of a total of 11 major peaks observed during this period, 2 occurred only in PM_{10}, 6 only in PM_{10} and 3 in both categories. All peaks occurred during 0900 UT and 1900 UT i.e. when the Sun was high. Peaks in PM_{10} category occurred in overcast conditions, in PM_1 category occurred under clear sky conditions and in both categories occurred when a cloud coverage of 4–8 octa started to decrease and changed to clear sky conditions within a period of a few hours. However, since all the peaks occurred in lull conditions when the wind speed dropped to almost zero, we do not rule out the occurrence of these peaks being associated with the local pollution from the Maitri station.

4.3. Number size distributions of aerosol particles

The number size distribution curves separately averaged for the whole data obtained in January and February, 2005 simultaneously obtained with the APS and SMPS, are plotted in Fig. 5. Table 2 shows the average modal parameters assuming the lognormal fit for curves in different size ranges (Jaenicke, 1993). Also plotted in Fig. 5, for comparison, are the size distribution curves of other investigators obtained at different coastal stations in Antarctica. The shape of our size distribution curves and the positions of maxima, as given in Table 2 are in general, agreement with other size distribution curves covering smaller size ranges.

There is much less scatter between different curves for the particles in the size range of 0.05–0.5 μm diameter as compared to the particles smaller and larger than this size range. The maxima in the accumulation and Aitken modes appear in most of the curves and show comparatively small variability in their positions. On the other hand, the nucleation mode maxima show large variability, both in size and in concentration of particles among different curves. Though, there are not many data-sets available for comparison, in the coarse particle size range, the agreement of our data with those of Radke and Lyons (1982) and Harvey et al. (1991) is reasonable. Further, although Deshpande and Kamra (2004) also observed the Aitken mode in the same size range in their measurements at Maitri, the present data with finer time-resolution step, precisely fix the positions of maxima and close their open-ended curves at small size-end due to unreliability of their instrument for measurements in this size range. Large scatter between different data-sets for the nucleation mode particles is presumably related to the variability in strength of different sources responsible for their origin and will be further discussed in Section 4.

4.4. Variability in different modes

An examination of our data with finer time-average step reveals that the hourly-averaged size distribution curves in each size range exhibit large variability from the monthly-averaged curves plotted

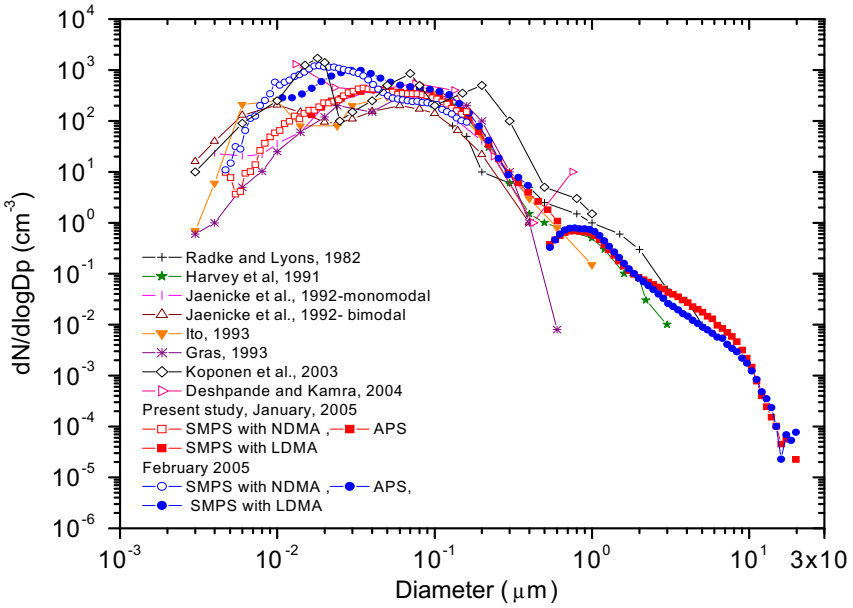

Fig. 5. Number size distribution curves averaged for the whole data simultaneously obtained with the APS and SMPS systems in different size categories during the months of January and February, 2005. Hollow and solid labels for the present study represent data obtained with the NDMA and APS/LDMA, respectively. Also shown, for comparison, are the number size distributions observed by various investigators at different coastal Antarctic stations.

Table 2
Modal parameters for the monthly-averaged curves in Fig. 5.

Period	Modal parameter	Nucleation mode (NM)	Aitken mode	Accumulation mode
January	N		243 ± 111	0.168 ± 0.084
	D_{gN}		0.089 ± 0.005	0.772 ± 0.023
	σ		1.343 ± 0.020	1.196 ± 0.003
February	N	330 ± 165	474 ± 255	0.185 ± 0.088
	D_{gN}	0.018 ± 0.002	0.030 ± 0.003	0.746 ± 0.031
	σ	1.491 ± 0.042	1.357 ± 0.022	1.187 ± 0.004

The standard deviation in each mode diameter represents its variability in all the curves for January/February.
N – total number concentration (cm^{-3}), D_{gN} – geometric mean diameter (μm), σ – geometric standard deviation of the size distribution.

in Fig. 5. Below, we discuss these deviations in different size ranges, with particular emphasis on the appearance of new modes or shifting of modes on smaller time-scales.

4.4.1. Coarse and accumulation modes

Throughout the period of our observations, the coarse mode particles normally exhibit a steep decrease in concentration with the increase in particle size. However, particles of >2 μm diameter often exhibit much larger variability in concentration than those of smaller particles on time-scale of an hour or less. When examined on hourly scale the coarse mode particles occasionally develop a maximum at 2.120 ± 0.296 (2.134 ± 0.327) μm in January (February) which continues to exist for several hours. Fig. 6 shows four mean curves each averaged separately from all the hourly-averaged monomodal or bimodal size distribution curves observed in January and February in our data. Numbers in parenthesis show the number of times such hourly-averaged curves have been observed and the standard deviation shows the variability of the mean mode diameter in all curves of similar type. Our APS measurements always show an accumulation mode at 0.702 ± 0.044 (0.820 ± 0.067) μm in January (February) which shifts to at 0.720 ± 0.056 (0.728 ± 0.070) μm in January (February) when the coarse mode maximum also appears (Table 3). Harvey et al. (1991) also showed almost similar size distribution of particles with large variability in concentrations of particles of >2 μm diameter which mostly consisted of salt particles. In our observations before January 16, 2005 when the atmospheric temperatures mostly remained above freezing and winds were >4–6 m s^{-1} the maximum at 2.120 ± 0.296/2.134 ± 0.327 μm was observed almost daily for a few hours. On the contrary, this maximum rarely appeared in February when inspite of high winds, the air temperatures decreased and remained below freezing for most part of the day. Further, concentration of particles of >2 μm diameter increased by about an order of magnitude during the periods when both coarse and accumulation modes appeared. So the process of stripping-off of liquid phase particles from the surface in strong wind conditions and their re-suspension in the atmosphere most probably contributes to the coarse particle concentration.

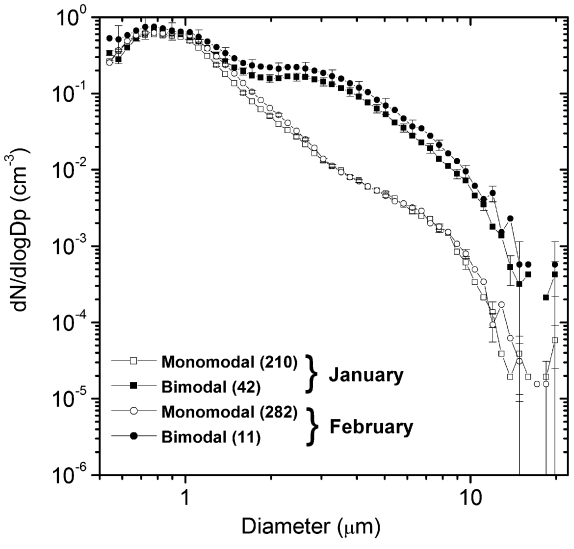

Fig. 6. Mean size distribution curves of monomodal (a) and bimodal (b) shapes computed from the hourly-averaged curves (as measured with the APS) of respective shapes observed during the period of January–February, 2005. Numbers in parenthesis show the number of aerosol size distribution curves used to compute the mean curve.

The coarse component of aerosol particles observed over coastal areas is known to be mainly contributed by the sea-salt particles generated by the wave-breaking process at sea surface and transported to the coast by winds (Blanchard, 1985). Consequently, sea-salt is usually the most abundant aerosol component at the coastal Antarctic sites (Hall and Wolff, 1998). Number size distributions of particles in our observations at Maitri are not much different from the measurements of Koponen et al. (2002) made at the Finnish station, Aboa, at a distance of about 150 km from the open ocean, which show that more than 70% of sea-salt lies in the PM_{10} category and mass size distribution of sea-salt shows a trimodal distribution with maxima at 0.5–1 μm, 2 μm and somewhere between 2 and 10 μm diameters. Large particles in the size range of 0.5–1 μm diameter, although found in concentrations of only ~0.15 cm^{-3}, dominate the aerosol mass. However, these are of great interest because they are likely to have been transported from long distances and precipitated onto the surface and thus incorporated in polar ice in varying rates. Ice-core analysis for such aerosols can show a connection with past changes in terrestrial climate (Petit et al., 1981; Bigler et al., 2006).

In absence of local sources, our observations of (i) low concentration of particles in coarse mode throughout the campaign period, (ii) occurrence of the coarse mode maxima at relatively small particle size, and (iii) very low concentrations of particles of >10 μm diameter are supported by the fact that- large particles in coarse mode are likely to settle down to the ground by sedimentation during their transit from sea to Maitri. The aerosol over Maitri will therefore get depleted of large particles.

4.4.2. Aitken I and Aitken II modes

Most of the PM_1 category particles suspended in the Antarctic troposphere are formed from oxidation of the Dimethyl Sulfide (DMS) emitted by the ocean and are known to show a seasonal variability at various coastal sites (Iwai, 1979; Ito and Iwai, 1981; Shaw, 1986; Jaenicke and Stingl, 1984; Jaenicke et al., 1992; Gras and Adriaansen, 1985; Ito, 1993) as well as at the South Pole (Hogan, 1975). Their prevalence in the sunlit months, suggests their production by the photochemical processes. Importance of Aitken mode particles is not only because they can act as cloud condensation nuclei (CCN) but also because they are intermediates between newly formed nucleation mode particles and the particles which can act as CCN. The present finer time-average data can be used in computations of the growth rates of nucleation mode particles to CCN sizes. Although the monthly-averaged size distribution curves for Aitken particles are monomodal, the hourly-averaged curves in our high resolution data can be both monomodal or bimodal in shape. Fig. 7 shows four mean curves each separately averaged from all monomodal and bimodal curves observed during the months of January and February. While the monomodal curve shows a maximum in Aitken mode at

Table 3
Modal parameters of different number size distributions plotted in Figs. 6, 7 and 8.

Figure No.	Size distribution	Modal parameters	Nucleation mode	Aitken mode I	Aitken mode II	Accumulation mode	Coarse mode
Fig. 5	Monomodal–January	N				0.140 ± 0.062	
		D_{gN}				0.702 ± 0.044	
		σ				1.186 ± 0.001	
	Monomodal–February	N				0.168 ± 0.083	
		D_{gN}				0.820 ± 0.067	
		σ				1.196 ± 0.002	
	Bimodal–January	N				0.148 ± 0.066	0.132 ± 0.085
		D_{gN}				0.720 ± 0.056	2.120 ± 0.296
		σ				1.183 ± 0.001	1.705 ± 0.006
	Bimodal–February	N				0.163 ± 0.085	0.158 ± 0.091
		D_{gN}				0.728 ± 0.070	2.134 ± 0.327
		σ				1.192 ± 0.002	1.686 ± 0.007
Fig. 6	Monomodal–January	N			104 ± 46		
		D_{gN}			0.080 ± 0.011		
		σ			1.368 ± 0.012		
	Monomodal–February	N			192 ± 73		
		D_{gN}			0.042 ± 0.014		
		σ			1.420 ± 0.017		
	Bimodal–January	N		306 ± 113	162 ± 58		
		D_{gN}		0.031 ± 0.004	0.075 ± 0.007		
		σ		1.166 ± 0.110	1.364 ± 0.008		
	Bimodal–February	N		398 ± 130	162 ± 58		
		D_{gN}		0.029 ± 0.004	0.088 ± 0.006		
		σ		1.383 ± 0.116	1.331 ± 0.006		
Fig. 7	a	N	335 ± 164		77 ± 28		
		D_{gN}	0.017 ± 0.002		0.089 ± 0.013		
		σ	1.409 ± 0.044		1.317 ± 0.003		
	b	N	497 ± 336	1082 ± 328			
		D_{gN}	0.010 ± 0.001	0.024 ± 0.004			
		σ	1.602 ± 0.021	1.352 ± 0.002			
	c	N	229 ± 168	196 ± 69	80 ± 28		
		D_{gN}	0.010 ± 0.001	0.023 ± 0.002	0.085 ± 0.004		
		σ	1.501 ± 0.054	1.410 ± 0.029	1.336 ± 0.007		

The standard deviation in each mode diameter represents its variability in the number of similar curves, illustrated in figures.

0.08 ± 0.011 (0.042 ± 0.014) μm in January (February), the bimodal curve shows two maxima as Aitken mode I at 0.031 ± 0.004 (0.029 ± 0.064) μm in January (February) and Aitken mode II at 0.075 ± 0.007 (0.088 ± 0.066) μm in January (February). Majority of size distributions in this size range are monomodal in January and bimodal in February. Observation of two maxima in Aitken mode might have been missed in previous observations at Antarctic coast because of the low resolution measurements. Supporting such a possibility, are several observations of multi-modal size distributions of Jaenicke et al. (1992) who noticed that averaging of distributions transforms them to a single-mode shape with the maximum between 0.03 and 0.09 μm because of varying locations of modes. However, their observations do not confirm a maximum at 0.01 μm as reported by Ito (1993). Since the gas-to-particle conversion processes produce particles of only 0.002–0.003 μm in size, Jaenicke et al. (1992) suggested that further studies are needed to explain the generation and growth of aerosols at Antarctica. Observation of both monomodal and bimodal size distribution in Aitken range in the present measurements suggest that the nucleation mode particles grow in size at two different rates by different processes, such as the condensation of low volatility vapour on hygroscopic or non-hygroscopic, or on charged or neutral fractions of particles under different atmospheric conditions (e.g. see many references in Kulmala et al., 2004). Our GICB measurements show that 15–25% of total number of aerosol particle in this size range may be charged (Siingh et al., in press). Alternately, the air masses arriving at Maitri originate from different sources and thus will have different aerosol compositions. Pant et al. (2010) show that downward transport of the new particles formed at higher altitudes, with the subsidence associated with the cyclonic storms revolving around the continent of Antarctica, can also grow and contribute to such particles.

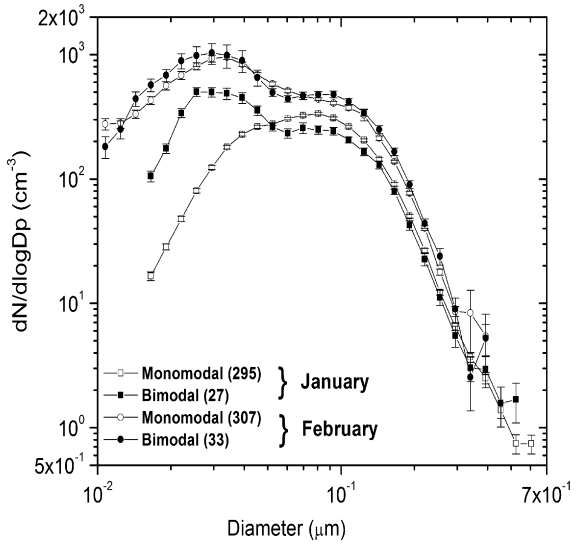

Fig. 7. Mean size distribution curves of monomodal (a) and bimodal (b) shapes computed from the hourly-averaged curves (as measured with the SMPS using LDMA) of respective shapes observed during the period of January–February, 2005. Numbers in parenthesis show the number of aerosol size distribution curves used to compute the mean curve.

Previous measurements of Jaenicke et al. (1992), Gras (1993) and Ito (1993) showed the presence of a broad mode below

0.1–0.2 μm accompanied by a nucleation mode below 0.02 μm diameter during the summer. However, Koponen et al. (2003) reported that the Aitken and accumulation modes are separately distinguishable in their measurements. The present measurements demonstrate that even Aitken mode particles can exhibit two modes. The maximum for Aitken mode I shows large variability in magnitude and sometimes even envelopes the maximum for Aitken mode II when the data is averaged over large ranges of the particle size/time. Observation of these additional modes might have been missed in previous measurements either because of the masking of detailed modal structure when the data is averaged over several weeks, or because of low particle size-resolution which is not enough to distinguish between two modes that lie close to each other.

4.4.3. Nucleation mode

Measurements of particles of 0.003–0.16 μm diameter were made only for short spells of time. The hourly-averaged size distribution curves obtained for these periods frequently show the presence of particles of <0.01 μm diameter. Although, concentration of such particles shows large variability with time, the maximum is observed mostly at ~0.01 μm or 0.017 μm diameters. Fig. 8 shows three types of mean size distribution curves averaged from the hourly-averaged curves observed during this period when the nucleation mode particles appear. In the first type, (curve a), the nucleation mode particles of >0.005 μm diameter are present and their concentration peaks at 0.017 μm. These particles are not of recent origin and further grow by condensation and coagulation processes to show a maximum in Aitken mode II range. In the second type (curve b), the nucleation mode distinctly appears at 0.01 μm and is accompanied with a maximum in Aitken mode I range. In the third case (curve c), though the nucleation mode still appears at 0.01 μm, it is accompanied with one maximum each in Aitken mode I and Aitken mode II ranges. During the periods when the nucleation mode particles appear, concentration of Aitken mode particles increases and the Aitken mode becomes prominent with total number concentrations reaching in the range of 10^3–10^4 cm^{-3}.

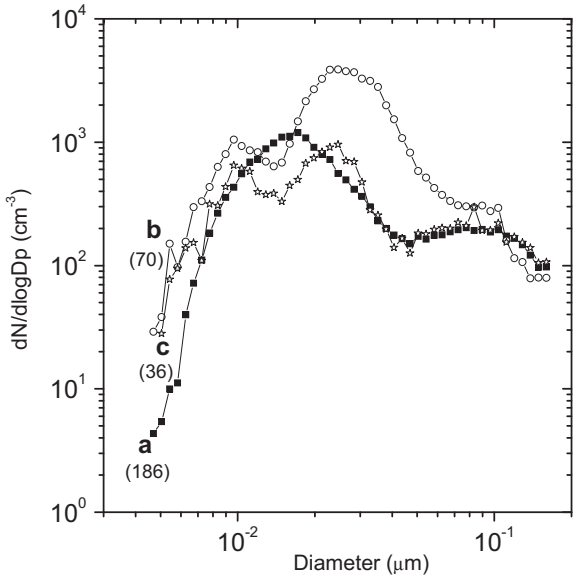

Fig. 8. Mean size distribution curves of monomodal (a), bimodal (b), and trimodal (c) shapes computed from the hourly-averaged curves (as measured with the SMPS using NDMA) of respective shapes observed during the period of January–February, 2005. Numbers in parenthesis show the number of aerosol size distribution curves used to compute the mean curve.

Since particles <0.005 μm diameter were practically never observed in our measurements and they need significant time to grow to this size, these are assumed to be transported from other places to Maitri. One possible source for these nuclei, as suggested by Ito (1993) and supported by Koponen et al. (2002), could be the free troposphere and their transport to the marine boundary layer under subsidence of cyclonic storms revolving around Antarctica. Our measurements made during cyclonic storms in the same expedition, strongly suggest the downward transport of nucleation particles formed in the outflow of storms, with the subsidence associated with the storms (Pant et al., 2010). These particles subsequently grow at a rate of 0.2–0.6 nm h^{-1} (Pant et al., 2010). Prevalence of nucleation mode at 0.017 μm in continental air mass shows that these particles are aged. The fact that the Aitken particle maximum is more prominent when nucleation mode appears suggests that nucleation mode particles grow, possibly by condensation of low volatility gases, cloud processes and/or by coagulation of particles to Aitken particle size (Hoppel et al., 1985). The processes of condensation and coagulation are then known to grow these particles to the size of accumulation mode particles (Whitby and Cantrell, 1976).

Modal parameters for various size distribution curves plotted in Figs. 6–8, are given in Table 3. While the positions of maxima for coarse, accumulation, Aitken and nucleation modes are almost fixed as shown in Table 3, their heights often vary from day to day and even from hour to hour. Particularly, the height of Aitken mode appreciably increases whenever nucleation mode appears. Large variability in nucleation mode particles can be contributed by both the variability in rate of their generation and/or by lower averaging statistics in our measurements.

Although, no organized attempts were made for measurements of particles of <0.003 μm diameter, GICB was manually operated in mobility-measuring mode on two days to get 8 mobility-spectra on January 17 and 4 mobility-spectra on February 18, 2005. These

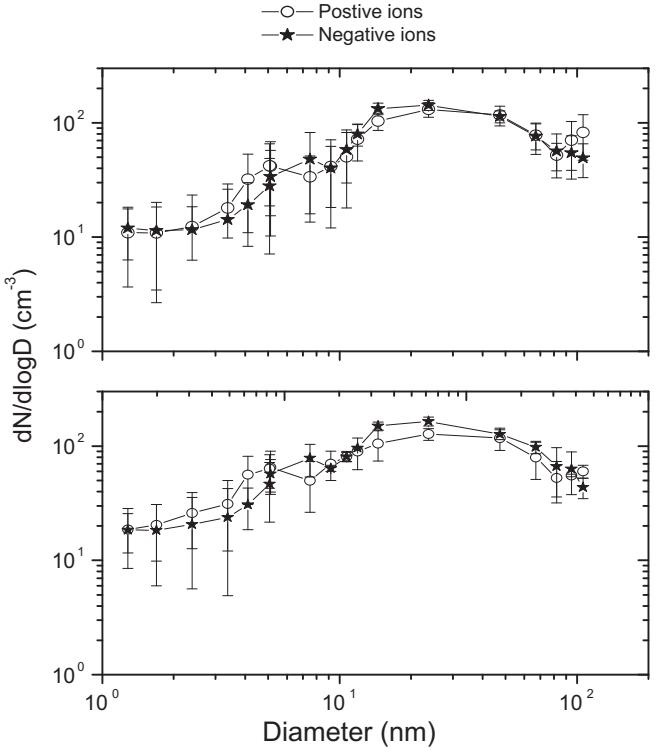

Fig. 9. Average size spectra for ions in the size range 0.4–109.5 nm on January 17, 2005 (upper panel) and February 18, 2005 (lower panel). Vertical bars show standard errors.

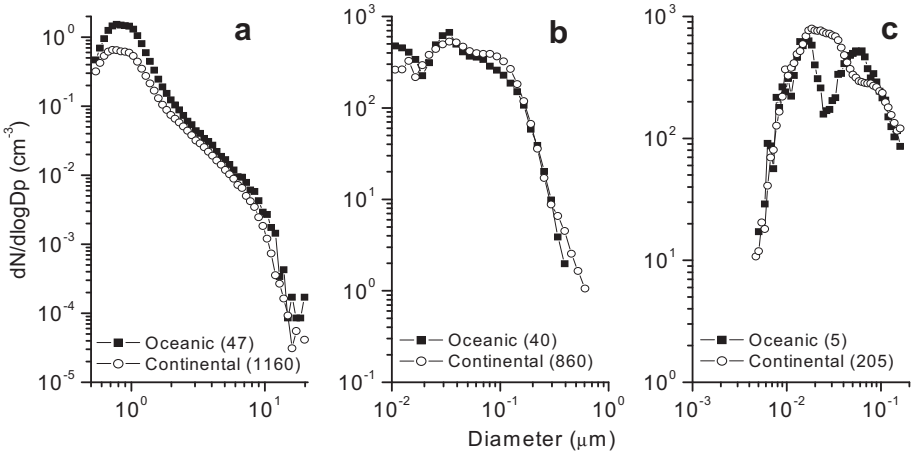

Fig. 10. Mean number size distribution curves for aerosol particles in different size ranges associated with the oceanic and continental air masses. Numbers in parenthesis show the number of hourly-averaged size distribution curves used to compute the mean curve.

measurements are described in detail by Siingh et al. (in press). Fig. 9 shows average size spectra of positive and negative ions in this size range, on both days. The ion size distributions always show a broad peak extending from 0.016 to 0.05 μm diameter for light large ions and indicate a peak beyond 0.08 μm for heavy large ions. A comparison of the data obtained from simultaneous measurements of ion spectra with GICB and aerosol size distributions with SMPS brings out several new features. For example the relative concentrations of ions and aerosols in the common range of measurements (0.016–0.107 μm diameter) strongly indicate the role of coagulation of charged particles in the evolutions of the ion and aerosol size distributions (Siingh et al., in press). Further, inspite of a new particle formation event on Days 49 (see also Fig. 3b) which produces a strong peak for nucleation mode aerosol particles, ion spectra do not show a corresponding peak, thereby indicating that only a part of the newly formed particles are charged (Siingh et al., in press).

5. Characteristics of aerosols in the oceanic and continental air masses

Air masses arriving at Maitri have been classified into the oceanic and continental air masses on the basis of 5-day back trajectories obtained for every hour during the period of observations. The aerosol size distribution curve corresponding to every 5-day back trajectory has been identified and all size distributions corresponding to the oceanic or continental air masses have been separately averaged. Fig. 10(a, b, and c) shows the number size distribution curves obtained with the APS and SMPS and averaged for the coastal and continental air masses. Concentration of the coarse mode particles has power-law size distribution. However, total number concentration of coarse mode particles is higher in oceanic air mass than in continental air mass (Fig. 10a). Such a trend is expected because of the origin of coarse mode particles by the bubble bursting process during high wind periods over sea and their transport to inland regions by horizontal winds (Blanchard, 1985).

Though accumulation mode is observed approximately at the same diameters in both types of air masses, particle concentration is about three times higher in oceanic than in continental air masses (Fig. 10a). In oceanic air masses, size distribution of particles in Aitken range is monomodal with a maximum at 0.039 μm. However, in continental air masses, it is bimodal with another maximum appearing at 0.085 μm (Fig. 10b). These features are presumably due to lower concentrations of SO_2 and cloud amounts in continental air masses which cause the growth of these particles by cloud processing (Hoppel et al., 1994).

Since our measurements with NDMA were made only for short periods, the size distribution for oceanic air masses plotted in Fig. 10c, is average of only 5 curves and is thus not statistically representative in this range. While size distribution curves for both continental and oceanic air masses show the presence of particles as small as 0.005 μm diameter, continental air masses show a maximum at 0.017 μm indicating the presence of aged particles. Several hourly-averaged size distribution curves in oceanic air masses show a sharp nucleation mode maximum at ~0.01 μm which may continue to exist for a few hours. Large temporal variability observed in nucleation mode maximum in our observations indicates that more than one nucleation process may be operating in the atmosphere (Kulmala et al., 2004).

6. Conclusions

Total number concentrations of PM_{10} and PM_1 particles in the size range of 0.003–20 μm diameter during the summer months of Janaury and February, 2005 at Maitri vary from 0.1 to 0.8 and from 100 to 2000 particles cm^{-3}, respectively. The monthly-averaged size distribution curves in our data are consistent with the previous measurements at various Antarctic coastal sites and always show one mode each in accumulation and Aitken size ranges. However, analysis of our data on hourly time-scale reveals that individual curves can frequently have one mode in each of the coarse, accumulation and nucleation size ranges and two modes in the Aitken size range. Total number concentration of particles in coarse mode is higher in oceanic than in continental air masses. Observations show that the oceanic air masses have nucleation mode at 0.01 μm and Aitken mode at 0.024 μm. However, continental air masses have nucleation mode at 0.017 μm. Multi-modal size distributions result when the oceanic and continental air masses intermix with each other on coastal sites. Observations indicate that nucleation mode particles are aged in continental air mass. However, such particles in oceanic air mass are likely to be transported from upper troposphere under subsidence associated with cyclonic storms revolving around the continent of Antarctica.

Acknowledgements

Authors express their gratitude to the National Centre for Antarctic and Ocean Research, Goa for participation in the 24th

Indian Scientific Expedition to Antarctica. The meteorological data provided by the India Meteorological Department is thankfully acknowledged. The authors gratefully acknowledge the NOAA Air Resources Laboratory (ARL) for the provision of the HYSPLIT transport and dispersion model and READY website (http://www.arl.noaa.gov/ready.html) used in this publication. One of us (AKK) acknowledge the support under INSA Senior Scientist Programme.

Appendix. Supplementary material

Supplementary data related to this article can be found at doi:10.1016/j.atmosenv.2011.06.028.

References

Albrecht, B.A., 1989. Aerosols, cloud microphysics and fractional cloudiness. Science 245, 1227–1230.
Bagnold, R.A., 1965. The Physics of Blown Sand and Desert Dunes. Methuen and Co. LTD, London II New Fetter Lane, E.C. 4.
Bigler, M., Rothlisberger, R., Lambert, F., Stocker, T.F., Wagenbach, D., 2006. Aerosol deposited in East Antarctica over the last glacial cycle: detailed apportionment of continental and sea-salt contributions. J. Geophys. Res. 111 (D08205). doi:10.1029/2005JD006469.
Blanchard, D.C., 1985. The oceanic production of atmospheric sea salt. J. Geophys. Res. 90, 961–963.
Bodhaine, B.A., DeLuisi, J.J., Harris, J.M., Houmere, P., Bauman, S., 1986. Aerosol measurements at the south pole. Tellus B 38, 223–225.
Charlson, R.J., Lovelock, J.E., Anreae, M.O., Warren, S.G., 1987. Oceanic phytoplankton, atmospheric sulphur, cloud albedo and climate. Nature 326, 655–661.
Charlson, R., Schwartz, S., Hales, J., Cess, R., Coakley Jr., R.J., Hansen, J., Hofmann, D., 1992. Climate forcing by anthropogenic aerosols. Science 255, 423–430.
Chylek, P., Coakley Jr., J.A., 1974. Aerosols and climate. Science 183, 75–77.
De Felice, T.P., Saxena, V.K., Yo, S., 1997. On the measurements of the cloud condensation nuclei at Palmer station, Antarctica. Atmos. Environ. 31, 4039–4044.
de la Mare, W.K., 1997. Abrupt mid-twentieth-century decline in Antarctic sea-ice extent from whaling records. Nature 389, 57–60.
Deshpande, C.G., Kamra, A.K., 2004. Physical properties of aerosols at Maitri, Antarctica. Proc. Indian Acad. Sci. (Earth Planet. Sci.) 113 (1), 1–25.
Dhanorkar, S., Kamra, A.K., 1991. Measurement of mobility spectrum and concentration of all atmospheric ions with a single apparatus. J. Geophys. Res. 96, 18671–18678.
Draxler, R.R., Hess, G.D., 1998. An overview of the HYSPLIT4 modeling system for trajectories, dispersion and deposition. Aust. Meteorol. Mag. 47, 295–308.
Draxler, R.R., Rolph, G.D., 2003. HYSPLIT (Hybrid Single-Particle Lagrangian Integrated Trajectory) Model Access via NOAA ARL READY. NOAA Air Resources Laboratory, Silver Spring, MD. Website. http://www.arl.noaa.gov/ready/hysplit4.html.
Fuchs, N.A., 1964. The Mechanics of Aerosols. Pergamon Press, p. 408.
Gras, J.L., 1993. Condensation nucleus size distribution at Mawson, Antarctica: microphysics and chemistry. Atmos. Environ. 27, 1417–1425.
Gras, J.L., Adriaansen, A., 1985. Concentration and size variation of condensation nuclei at Mawson, Antarctica. J. Atmos. Chem. 3, 96–103.
Hall, J.S., Wolff, E.W., 1998. Causes of seasonal and daily variations in aerosol sea-salt concentrations at a coastal Antarctic station. Atmos. Environ. 32, 3669–3677.
Hara, K., Osada, K., Kido, M., Hayashi, M., Matsunaga, K., Iwasaka, Y., Yamanouchi, T., Hashida, G., Fukatsu, T., 2004. Chemistry of sea-salt particles and inorganic halogen species in Antarctic regions: compositional differences between coastal and inland stations. J. Geophys. Res. 109 (D20208). doi:10.1029/2004JD004713.
Hara, K., Osada, K., Kido, M., Matsunaga, K., Iwasaka, Y., Hashida, G., Yamanouchi, T., 2005. Variations of constituents of individual sea-salt particles at Syowa station, Antarctica. Tellus B 57, 230–246. doi:10.1111/j.1600-0889.2005.00142.x.
Hara, K., Iwasaka, Y., Wada, M., Ihara, I., Shiba, H., Osada, K., Yamanouchi, T., 2006. Aerosol constituents and their spatial distribution in the free troposphere of coastal Antarctic regions. J. Geophys. Res. 111 (D15216). doi:10.1029/2005JD006591.
Harvey, M.J., Fisher, G.W., Lechner, I.S., Issac, P., Flower, N.E., Dick, A.L., 1991. Summertime aerosol measurement in the Ross sea region of Antarctica. Atmos. Environ. 25, 569–580.
Hogan, A.W., 1975. Antarctic aerosols. J. App. Met 14, 550–559.
Hogan, A.W., 1979. Meteorological transport of particulate material to the south polar plateau. J. Appl. Meteorol. 18, 741–749.
Holland, M.M., Bitz, C.M., Tremblay, B., 2006. Future abrupt reductions in the summer Arctic sea ice. Geophys. Res. Lett. 33 (L23503). doi:10.1029/2006GL028024.
Hoppel, W.A., Fitzgerald, J.A., Larson, R.E., 1985. Aerosol size distributions in air masses advecting off the East Coast of the United States. J. Geophys. Res. 90, 2365–2379.
Hoppel, W.A., Frick, G.M., Fitzgerald, J.W., Larson, R.E., 1994. Marine boundary layer measurements of new particle formation and the effect which non-precipitating clouds have on the aerosol size distribution. J. Geophys. Res. 99, 14442–14459.
Ito, T., 1993. Size distribution of Antarctic submicron aerosols. Tellus B 45, 145–159.
Ito, T., Iwai, K., 1981. On the sudden increase in the concentration of Aitken particles in the Antarctic atmosphere. J. Meteorol. Soc. Jpn. 59, 262–271.
Iwai, K., 1979. Concentration of Aitken particles observed at Syawo station, Antarctica (in Japanese). Nankyoku Shiryo 67, 172–179.
Jaenicke, R., 1993. Tropospheric aerosols. In: Hobbs, P.V. (Ed.), Aerosol-Cloud-Climate Interactions. Academic Press, San Diego, pp. 1–31.
Jaenicke, R., Stingl, J., 1984. Aitken particle size distribution in Antarctica. In: Proceedings of International Conference on Aerosols and Ice Nuclei. University of Budapest Press, Budapest, Hungary.
Jaenicke, R., Dreiling, V., Lehmann, E., Koutsenoguii, P.K., Stingl, J., 1992. Condensation nuclei at the German Antarctic station 'Georg von Neumayer'. Tellus 44B, 311–317.
Jourdain, B., Legrand, M., 2001. Seasonal variations of atmospheric dimethylsulfide, dimethyl20 sulfoxide, sulfur dioxide, methanesulfonate, and non-sea-salt sulfate aerosols at Dumont d'Urville (coastal Antarctica) (December 1998 to July 1999). J. Geophys. Res. 106, 14391–14408.
Jourdain, B., Preunkert, S., Cerri, O., Castebrunet, H., Udisti, R., Legrand, M.R., 2008. Year round record of size-segregated aerosol composition in central Antarctica (Concordia station): implications for the degree of fractionation of sea-salt particles. J. Geophys. Res. 113 (D14308). doi:10.1029/2007JD009584.
Kerminen, V.-M., Teinila, K., Hillamo, R., 2000. Chemistry of sea-salt particles in the summer Antarctic atmosphere. Atmos. Environ. 34, 2817–2825.
Koponen, I.K., Virkkula, A., Hillamo, R., Kerminen, V.-M., Kulmala, M., 2002. Number size distributions and concentrations of marine aerosols: observations during a cruise between the English Channel and the coast of Antarctica. J. Geophys. Res. 107 (D24), 4753. doi:10.1029/2002JD002533.
Koponen, I.K., Virkkula, A., Hillamo, R., Kerminen, V.-M., Kulmala, M., 2003. Number size distributions and concentrations of the continental summer aerosols in Queen Maud Lad, Antarctica. J. Geophys. Res. 108 (D18), 4587. doi:10.1029/2002JD002939.
Kulmala, M., Vehkamaki, H., Petaja, T., Dal Maso, M., Lauri, A., Kerminen, V.-M., Birmili, W., McMurry, P.H., 2004. Formation and growth rates of ultrafine atmospheric particles: a review of observations. J. Aerosol Sci. 35, 143–176.
Lal, M., Kapoor, R.K., 1989. Certain meteorological features of submicron aerosols at Schirmacher oasis, East Antarctica. Atmos. Environ. 23, 803–808.
Mazzera, D.M., Lowenthal, D.H., Chow, J.C., Watson, J.G., Grubisic, V., 2001. PM_{10} measurements at McMurdo station, Antarctica. Atmos. Environ. 35, 1891–1902.
Minikin, A., Legrand, M., Hall, J., Wagenbach, D., Kleefeld, C., Wolff, E., Pasteur, E.C., Ducroz, F., 1998. Sulfur-containing species (sulfate and methanesulfonate) in coastal Antarctic aerosol and precipitation. J. Geophys. Res. 103, 10975–10990.
Pant, V., Despande, C.G., Kamra, A.K., 2008. On the aerosol number concentration-wind speed relationship during a severe cyclonic storm over South Indian Ocean. J. Geophys. Res. 113 (D02206). doi:10.1029/2006JD008035.
Pant, V., Siingh, Devendraa, Kamra, A.K., 2010. Concentrations and size distributions of aerosol particles at Maitri during the passage of cyclonic storms revolving around the continent of Antarctica. J. Geophys. Res. 115 (D17202). doi:10.1029/2009JD013481.
Park, J., Sakurai, H., Vollmers, K., McMurry, P.H., 2004. Aerosol size distribution measured at south pole during ISCAT. Atmos. Environ. 38, 5493–5500.
Parish, T.R., 1988. Surface wind over the Antarctic continent: a review. Rev. Geophys. 26, 169–180.
Peters, T.M., Ott, D., O'Shaughnessy, P.T., 2006. Comparison of the Grimm 1.108 and 1.109 portable aerosol spectrometer to the TSI 3321 aerodynamic particle sizer for dry particles. Ann. Occup. Hyg. 50 (8), 843–850.
Petit, J.R., Briat, M., Royer, A., 1981. Ice age aerosol content from East Antarctic ice core samples and past wind strength. Nature 293, 391–394.
Radke, L.F., Lyons, J.H., 1982. Airborne measurements of particles in Antarctica. In: 2nd Symposium on Composition of the Non-urban Troposphere. American Met. Soc., Massachusetts USA, pp. 159–163.
Randles, C.A., Russell, L.M., Ramaswamy, V., 2004. Hygroscopic and optical properties of organic sea salt aerosol and consequences for climate forcing. Geophys. Res. Lett. 31 (L16108). doi:10.1029/2004GL020628.
Rankin, A., Wolff, E., 2003. A year-long period record of size-segregated aerosol composition at Halley, Antarctica. J. Geophys. Res. 108, 4775. doi:10.1029/2003JD003993.
Samson, J.A., Barnard, S.C., Obremski, J.S., Riley, D.C., Black, J.J., Hogan, A.W., 1990. On the systematic variation in surface aerosol concentration at the south pole. Atmos. Res. 25, 385–396.
Savoie, D.L., Prospero, J.M., Larsen, R.J., Huang, F., Izaguirre, M.A., Huang, T., Snowdon, T.H., Custals, L., Sanderson, C.G., 1993. Nitrogen and sulfur species in Antarctic aerosols at Mawson, Palmer station and Marsh (King George Island). J. Atmos. Chem. 17 (2), 95–122.
Schwartz, J., Dockery, D.W., Neas, L.M., 1996. Is daily mortality associated specifically with fine particles? J. Air Waste Manage. Assoc. 46, 927–939.
Shaw, G.E., 1986. On the physical properties of aerosol at Ross island, Antarctica. J. Aerosol. Sci. 17, 937–945.
Shaw, G.E., 1988. Antarctic aerosols: a review. Rev. Geophys. 26, 89–112.
Siingh, Devendraa, Pawar, S.D., Gopalakrishnan, V., Kamra, A.K., 2005. Measurements of ion concentrations and conductivity over the Arabian Sea during the ARMEX. J. Geophys. Res. 110 (D18207). doi:10.1029/2005JD005765.

Siingh, Devendraa, Pant, V., Kamra, A.K., 2007. Measurements of positive ions and air-Earth current density at Maitri, Antarctica. J. Geophys. Res. 112 (D13212). doi:10.1029/2006JD008101.

Siingh, Devendraa, Pant, V., Kamra, A.K. The ion-aerosol interactions from the ion mobility and aerosol particle size distribution measurements on January 17 and February 18 2005 at Maitri, Antarctica – A case study. J. Earth System Sc., in press.

Squires, P., 1958. The microstructure and colloidal stability of warm clouds. I. The 1 relation between structure and stability. Tellus 10, 256–271.

Tammet, H., 1995. Size and mobility distribution of nanometer particles, cluster and ions. J. Aerosol Sci. 26, 459–475.

Teinila, K., Kerminen, V.-M., Hillamo, R., 2000. A study of size-segregated aerosol chemistry in the Antarctic atmosphere. J. Geophys. Res. 105, 3893–3904.

Tomasi, C., et al., 2007. Aerosols in polar regions: a historical overview based on optical depth and in situ observations. J.Geophys. Res. 112 (D16205). doi:10.1029/2007JD008432.

Twomey, S.A., 1974. Pollution and the planetary albedo. Atmos. Environ. 8, 1251–1256.

Virkkula, A., Teinila, K., Hillamo, R., Kerminen, V.-M., Saarikoski, S., Aurela, M., Viidanoja, J., Paatero, J., Koponen, I.K., Kulmala, M., 2006. Chemical composition of boundary layer aerosol over the Atlantic Ocean and at an Antarctic site. Atmos. Chem. Phys. 6, 3407–3421.

Wagenbach, D., Curroz, F., Mulvaney, R., Keck, L., Minikin, A., Legrand, M., Hall, J.S., Wolff, E.W., 1998. Sea-salt aerosol in coastal Antarctic regions. J. Geophys. Res. 103, 10961–10974.

Whitby, K.T., Cantrell, B.K., 1976. Atmospheric Aerosols: Characteristics and Measurement. International Conference on Environmental Sensing and Assessment (ICESA). Institute of Electrical and Electronic Engineers (IEEE), Las Vegas, NV. September 14–19, 1976.

Wolff, E., Rankin, A., Roethlisberger, R., 2003. An ice core indicator of Antarctic sea ice production? Geophys. Res. Lett. 30, 2158. doi:10.1029/2003GL018454.

Yamazaki, K., Okada, K., Iwasaka, Y., 1989. Where do aerosol particles in the Antarctic upper troposphere come from? A case study in January 1983. J. Meteorol. Soc. Jpn. 67, 889–906.